Importance of oceanic heat uptake in transient climate change

Ronald J. Stouffer,[1] Joellen Russell,[2,3] and Michael J. Spelman[1]

Received 15 June 2006; revised 13 July 2006; accepted 20 July 2006; published 2 September 2006.

[1] The impact of the differences in the oceanic heat uptake and storage on the transient response to changes in radiative forcing is investigated using two newly developed coupled atmosphere-ocean models. In spite of its larger equilibrium climate sensitivity, one model (CM2.1) has smaller transient globally averaged surface air temperature (SAT) response than is found in the second model (CM2.0). The differences in the SAT response become larger as radiative forcing increases and the time scales become longer. The smaller transient SAT response in CM2.1 is due to its larger oceanic heat uptake. The heat storage differences between the two models also increase with time and larger rates of radiative forcing. The larger oceanic heat uptake in CM2.1 can be traced to differences in the Southern Ocean heat uptake and is related to a more realistic Southern Ocean simulation in the control integration. **Citation:** Stouffer, R. J., J. Russell, and M. J. Spelman (2006), Importance of oceanic heat uptake in transient climate change, *Geophys. Res. Lett.*, *33*, L17704, doi:10.1029/2006GL027242.

1. Introduction

[2] The time dependent or transient climate change can be thought of as being controlled by two global, large-scale parameters: the equilibrium climate sensitivity and the oceanic heat uptake [e.g., *Hansen et al.*, 1984; *Cubasch et al.*, 2001; *Raper et al.*, 2002]. Conventionally, the equilibrium climate sensitivity is defined as the equilibrium global surface air temperature change for a doubling of the atmospheric carbon dioxide concentration. Many times it is also expressed as a temperature change per W/m^2 change in radiative forcing. In modeling experiments, it is often estimated using an AGCM coupled to a mixed layer ocean (or slab) model which assumes no changes in oceanic heat transports. Normally one would expect a model with a larger climate sensitivity to have a larger transient climate response, except as discussed below.

[3] The oceanic heat uptake is directly related to the change in the amount of heat stored in the world oceans. As the radiative forcing of the planet changes, the forcing and also the feedbacks important in determining the climate sensitivity operate to change the surface temperature. The oceans act to buffer the temperature change in that some of the heat resulting from the radiative forcing changes is taken up by the oceans. This means at any point in time when the climate is adjusting to the radiative forcing changes, the surface temperature changes are smaller than what would occur if the oceans had a small heat capacity.

[4] *Hansen et al.* [1984] suggested that there is a relationship between climate sensitivity and oceanic heat uptake such that the larger the climate sensitivity, the larger the amount of oceanic heat uptake due to the interplay between the radiative damping of the planet and the storage of heat in the ocean. This relationship implies that the transient climate response [*Cubasch et al.*, 2001] will have a smaller spread among AOGCM results than implied by the spread of the climate sensitivities alone. *Raper et al.* [2002] analyzing a suite of AOGCM models found that the relationship suggested by Hansen et al. is seen in climate model projections used for the 3rd IPCC assessment.

[5] Here we use two versions of the newly developed GFDL (Geophysical Fluid Dynamics Laboratory/NOAA) climate models to further investigate the relationship between the climate sensitivity and the oceanic heat uptake. In one model, CM2.0, the SH atmosphere wind maximum is located too far north distorting the Southern Ocean simulation in the model [*Russell et al.*, 2006a]. In the second model, CM2.1, the atmospheric wind maximum is located much closer to its observed position, leading to a much more realistic Southern Ocean simulation in the model [*Russell et al.*, 2006a]. *Russell et al.* [2006b] show that this difference in the control simulations of the two AOGCMs has a large impact on the oceanic heat and implied carbon uptakes in a future radiative forcing scenario. Here we extend the analysis of the heat uptake and demonstrate that this difference has a large impact on the surface temperature response in all the perturbation integrations run with these models in support of the IPCC 4th Assessment process.

2. Model Description and Experimental Design

[6] The AOGCMs used in this study are described by *Delworth et al.* [2006] and the references therein. The oceanic components of the models are described by *Gnanadesikan et al.* [2006]. Only a short model description is given here. The reader is encouraged to look in those papers for further details on the model construction.

[7] The main difference between CM2.0 and CM2.1 is found in the atmospheric component. CM2.0 uses a B-grid dynamical core to compute the advection terms while CM2.1 uses the so-called finite volume core [*Delworth et al.*, 2006]. Both models use a finite difference grid that is about 2° of latitude in the horizontal with 24 unevenly spaced grid points in the vertical. Both models simulate the diurnal and seasonal cycles. Near state of the art physical parameterizations are used to mimic sub-grid scale processes too small to be resolved by the grid (see GAMDT 2004 for more details).

[1]Geophysical Fluid Dynamics Laboratory, Princeton, New Jersey, USA.
[2]Atmospheric and Oceanic Sciences Program, Princeton University, Princeton, New Jersey, USA.
[3]Now at Biogeochemical Dynamics Laboratory, Department of Geosciences, University of Arizona, Tucson, Arizona, USA.

0094-8276/06/2006GL027242$05.00

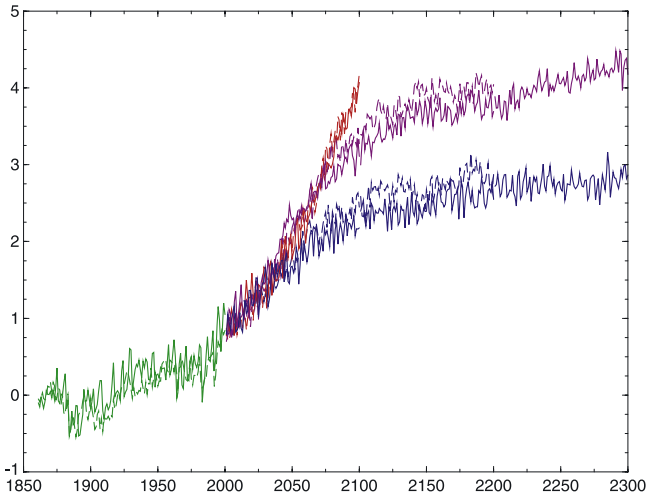

Figure 1. Time series of globally averaged surface air temperature (°K) from the various integrations. The anomaly is computed from the time average of the first 20 years of the historical integration. CM2.1 results are indicated by solid lines, CM2.0 by dashed lines. The line color indicates the type of integration: historical – green, A2 – red, A1B – purple, B1 – blue.

[8] The sea ice component is identical in both model versions. It allows leads in a given grid box and predicts ice thicknesses, concentrations and open water fraction using 5 sea ice thickness categories. The sea ice moves in response to the ocean currents and wind stress. Ice stresses and rheology are also considered in the prediction of ice movement. For more details see *Winton* [2000].

[9] The ocean component of both models includes a true free surface which allows fresh water fluxes to change the ocean surface elevation. Sub-grid mixing processes are simulated using the KPP scheme, GM and diffusion of tracers along isopycnals. The grid used has a horizontal spacing of 1° of latitude (finer in the tropics) and 50 vertical levels. Flux adjustments are not needed in either model to maintain a stable, realistic climate.

[10] One of the important differences between CM2.0 and CM2.1 is that CM2.1 oceanic component uses a substantially smaller value for the oceanic horizontal viscosity in the extratropics. This results in a stronger subpolar gyre circulation in the North Atlantic, with associated stronger poleward heat transports and reduced sea ice in the North Atlantic, including the Labrador Sea. Oceanic convection is also enhanced in the Labrador Sea in CM2.1 relative to CM2.0, possibly an important factor in understanding their differing responses to increasing greenhouse gases [*Stouffer et al.*, 2006].

[11] The integrations presented here were performed in support of the IPCC Fourth Assessment Report (AR4) due to be published in 2007. Much of the data obtained from these integrations is available at a PCMDI web site (https://esg.llnl.gov:8443/index.jsp) and at a GFDL web site (http://nomads.gfdl.noaa.gov/CM2.X) [*GFDL Global Atmospheric Model Development Team*, 2004]. Details on the input radiative forcing scenarios used in these integrations are given by *Knutson et al.* [2006].

3. Results

[12] Before discussing the results of the transient integrations, we present the climate sensitivities in the two models. The equilibrium climate sensitivity to a doubling of the atmospheric CO_2 concentration obtained using an AGCM coupled to a mixed layer ocean (or slab) model is 2.9K (globally averaged surface air temperature change) for CM2.0 and 3.4K for CM2.1 [*Stouffer et al.*, 2006]. As discussed in the Introduction, one would normally expect the transient responses to be larger in CM2.1 when compared to CM2.0 due to the larger climate sensitivity. However as noted by *Hansen et al.* [1984] and *Raper et al.* [2002], one would also expect the oceanic heat uptake to be larger in CM2.1 due to its larger climate sensitivity, somewhat compensating for the larger climate sensitivity.

[13] In all the transient integrations performed for the AR4 process, the globally averaged surface air temperature (SAT) response obtained for CM2.1 is smaller than that found in CM2.0 (Figure 1). This is contrary to what would be expected from the equilibrium climate sensitivity alone. One also sees that the difference in the SAT response between the two model results (CM2.1 and CM2.0) increases with time. During the historical integration (1860 to 2000), the difference between the model results is quite small, but by present day and into the future, the CM2.1 response is consistently smaller than the response found in the CM2.0 results. These differences are discussed below.

[14] It is also worth noting that during the period beyond 2100, the radiative forcing is held constant at the 2100 levels for the A1B and B1 integrations. These results are used to investigate the issue of stabilization of the climate. During this period, there is a small warming trend in both models using both scenarios. The slow continued warming after the radiative forcing is held constant, points to the long time scales of the climate response [*Hansen et al.*, 1985; *Stouffer*, 2004; *Meehl et al.*, 2005].

[15] An interesting question is if the smaller globally averaged SAT response in CM2.1 when compared to CM2.0 leads to a different pattern in the SAT response. The pattern of SAT response computed by averaging the response during the years 2081 to 2100 in the 3 SRES scenarios [*Nakicenovic and Swart*, 2000] used here is very similar between the two models (Figure 2). In both models, the warming is largest in high northern latitudes. The warming over the continents tends to be larger than that over the adjacent oceans. The eastern tropical Pacific tends to warm more than the western tropical Pacific Ocean, leading to a shift in the Walker circulation [*Vecchi et al.*, 2006]. The Southern Ocean tends to have a minimum in the warming due to the deep mixing of heat into the ocean in this region. Most of the changes described above have been documented in earlier AOGCM results [*Manabe et al.*, 1991; *Cubasch et al.*, 2001; *Dai et al.*, 2005].

[16] When comparing the CM2.1 response (Figure 2 top row) to the CM2.0 results (Figure 2 bottom row), the magnitude of the response is smaller in CM2.1 with the patterns of the response being very similar. The similarity of the response patterns discussed above is found in the difference maps for other time periods and forcing scenarios not shown. The cooling in the N Atlantic (particularly near the Labrador Sea) and in the Southern Ocean seems more

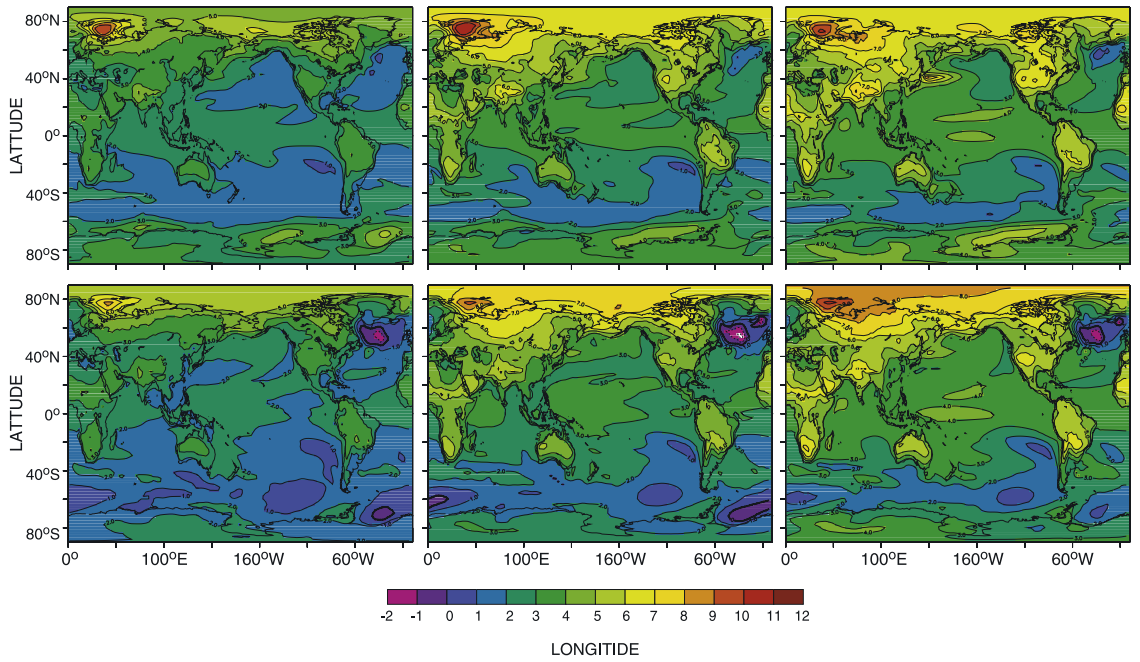

Figure 2. Surface air temperature difference, perturbation integration minus the 1860 control integration (°K). Results from the perturbation integration, years 2081–2100, minus the 100 year time average from the 1860 control: (Top row) CM2.0, (Bottom row) CM2.1, B1 (Left column), A1B (center), A2 (Right).

intense in CM2.1. The more intense Labrador Sea cooling in CM2.1 results from the shutdown of oceanic convection in this region [*Stouffer et al.*, 2006].

[17] As noted above, the smaller SAT response in CM2.1 is due to its larger ocean heat uptake. The time series of volume averaged oceanic temperature is used as a surrogate for heat storage here. Only the differences from the respective pre-industrial (1860) control integrations are shown. In both models (Figure 3), there is a relatively large decrease in the heat content just after the Krakatau eruption (year 1883). These negative anomalies persist well into the 20th century in both models. *Delworth et al.* [2005] and *Gleckler et al.* [2006] give more details on the impact of the Krakatau eruption on climate and on the subsurface ocean temperatures in particular. Near present day, the heat storage changes in CM2.1 are consistently larger than those seen in CM2.0. As time advances, the heat storage differences between the models become even larger. The greatly increased oceanic heat storage in CM2.1 is responsible for the smaller temperature increases.

[18] The oceanic heat uptake is largest in the middle to high latitudes of each hemisphere (Figure 4, top). The heat uptake in CM2.1 is larger than CM2.0 in middle and high latitudes of the NH and poleward shifted in the Southern Ocean. The ocean transports heat so that the oceanic heat storage can occur at different locations than the heat uptake (compare Figure 4 (top) and 4 (bottom)). In both models, the Southern Ocean is responsible for much of the oceanic heat storage in the transient integrations, with the tropics contributing much of the remaining part (Figure 4, bottom). In CM2.1, the Southern Ocean maximum is even larger than in CM2.0 and is located poleward of the CM2.0 maximum. This difference is due to the location of the Southern Hemisphere atmospheric jet. As described in *Russell et al.* [2006b], the SH atmospheric jet in CM2.1 is located poleward of the CM2.0 position. Its location CM2.1 is also much more realistic when compared to observations. The more realistic placement of the SH jet, allows much more of the volume of the Southern Ocean to be in contact with the atmosphere on decadal time scales, increasing the potential for larger heat storage changes through changes in the sensible and latent heat fluxes in the CM2.1 model. In both models, the SH atmospheric jet shifts poleward during the

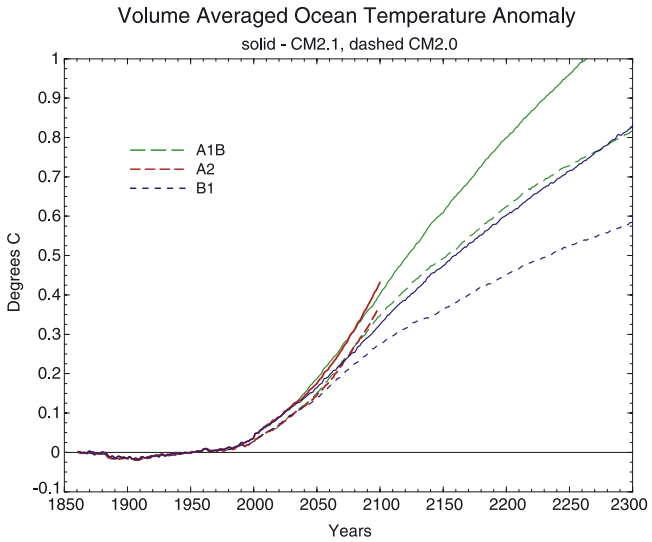

Figure 3. Time series of volume averaged ocean temperature difference (°K) for the various integrations minus the control. CM2.1 results are indicated by solid lines, CM2.0 by dashed lines. The line color indicates the type of integration: historical – blue, A2 – red, A1B – green, B1 – blue.

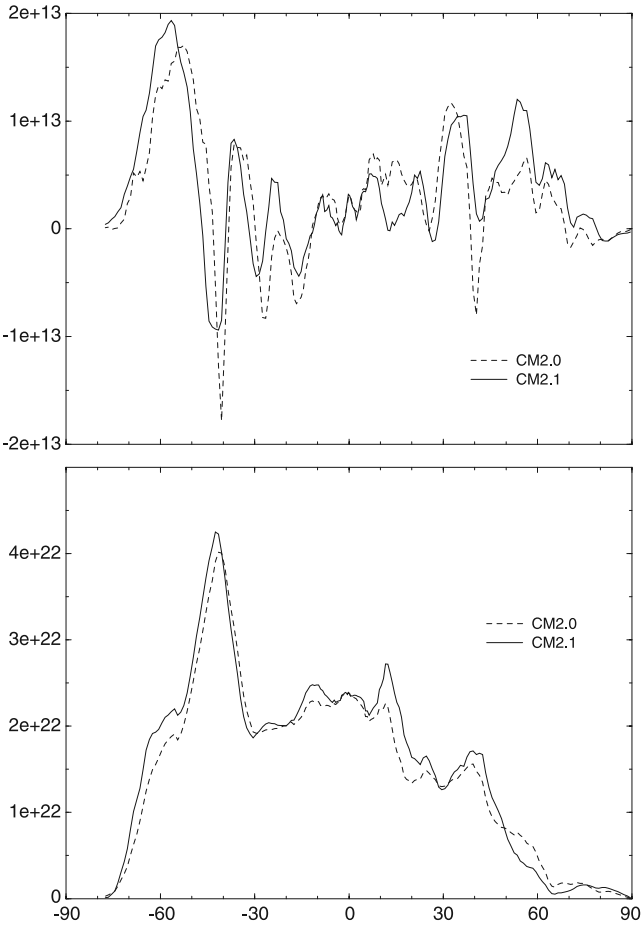

Figure 4. (top) Zonal sum of the total heat flux difference (watts), SRES A1B minus control, across the ocean surface (positive values indicate heating of the ocean). This difference is computed from 100 year time averages (2001–2100). (bottom) Latitude plot of the change in the oceanic heat content, years 2081 to 2100 in the SRES A1B integration minus a century time average in the control. The units are joules per degree latitude. In both plots, the solid line is CM2.1 data, dashed is CM2.0.

transient integrations, increasing heat storage in the Southern Ocean. However, this increase is larger in CM2.1 when compared to CM2.0.

4. Conclusion

[19] This paper again demonstrates the importance of oceanic heat uptake and storage in understanding transient response. This is not a new result. What is new and interesting is the impact of the differences in oceanic heat uptake on the transient response of the two models. The atmospheric jet placement and strength in CM2.1 is more realistic relative to CM2.0, which leads to a much more realistic Southern Ocean simulation in the control integrations and brings a much larger volume of water into contact with the atmosphere on decadal time scales [*Russell et al.*, 2006b]. The larger effective oceanic heat capacity in the CM2.1 control integration leads to a larger change in the oceanic heat storage in the transient integrations.

[20] While poorly located north of the observed position, the location of the SH atmospheric jet in CM2.0 is not atypical of the current state-of-the-art climate models which are being used in the AR4 report [*Russell et al.*, 2006a]. The location of the SH jet and associated Southern Ocean simulation is much more realistic in CM2.1. This fact could lead one to speculate that the oceanic heat uptake in CM2.1 is also more realistic.

[21] The larger heat uptake in CM2.1 leads to a smaller SAT change in response to radiative forcing changes. However, it also implies a larger oceanic temperature change. Since globally averaged steric sea level rise is closely linked to the changes in the volume averaged ocean temperature, the larger oceanic heat uptake also implies a larger steric sea level rise in CM2.1.

[22] In addition to the heat, carbon is also being taken up by the oceans in the present climate. A larger carbon uptake by the oceans would likely be linked to the larger heat uptake [*Russell et al.*, 2006b]. As was the case for the heat uptake, a larger carbon uptake would also imply smaller SAT changes because of a smaller increase in atmospheric CO_2 concentrations (although not modeled in this study). However the larger carbon uptake by the oceans would also lead to a lower pH, all other things being equal. The lower pH may have large, adverse impacts on the oceanic biology [*Feely et al.*, 2004]. This discussion of the possible carbon changes needs to be tempered with the realization that the biological changes themselves could greatly impact any carbon budget changes. The biological responses to a warming climate are not well known or understood [*Sarmiento et al.*, 1998; *Friedlingstein et al.*, 2003] and are the subject of future investigations.

[23] **Acknowledgments.** The authors thank Keith Dixon and Isaac Held for many helpful discussions. The authors also thank Tom Delworth, Tom Knutson, Jerry Meehl and Aiguo Dai for reviewing earlier versions of this paper.

References

Cubasch, U., et al. (2001), Projections of future climate change, in *Climate Change 2001: The Scientific Basis: Contribution of Working Group I to the Third Assessment Report of the Intergovernmental Panel on Climate Change*, edited by J. T. Houghton et al., 526–582, Cambridge Univ. Press, New York.

Dai, A., A. Hu, G. A. Meehl, W. M. Washington, and W. G. Strand (2005), Atlantic thermohaline circulation in a coupled model: Unforced variations vs. forced changes, *J. Clim.*, *18*, 3270–3293.

Delworth, T. L., V. Ramaswamy, and G. L. Stenchikov (2005), The impact of aerosols on simulated ocean temperature and heat content in the 20th century, *Geophys. Res. Lett.*, *32*, L24709, doi:10.1029/2005GL024457.

Delworth, T. L., et al. (2006), GFDL's CM2 global coupled climate models: part 1: Formulation and simulation characteristics, *J. Clim.*, *19*, 643–674.

Feely, R. A., C. L. Sabine, K. Lee, W. Berelson, J. Kleypas, V. J. Fabry, and F. J. Millero (2004), Impact of anthropogenic CO_2 on the $CaCO_3$ system in the oceans, *Science*, *305*, 362–366.

Friedlingstein, P., J. L. Dufresne, P. M. Cox, and P. Rayner (2003), How positive is the feedback between climate change and the carbon cycle?, *Tellus, Ser. B*, *55*, 692–700.

GFDL Global Atmospheric Model Development Team (2004), The new GFDL global atmosphere and land model AM2/LM2: Evaluation with prescribed SST simulations, *J. Clim.*, *17*, 4641–4673.

Gleckler, P., T. M. L. Wigley, B. D. Santer, J. M. Gregory, K. AchutaRao, and K. E. Taylor (2006), Krakatoa's signature persists in the ocean, *Nature*, *439*, 675, doi:10.1038/439675a.

Gnanadesikan, A., et al. (2006), GFDL's CM2 Global Coupled Climate Models: part 3: The baseline ocean simulation, *J. Clim.*, *19*, 675–697.

Hansen, J., A. Lacis, D. Rind, G. Russell, P. Stone, I. Fung, R. Ruedy, and J. Lerner (1984), Climate sensitivity: Analysis of feedback mechanisms, in *Climate Processes and Climate Sensitivity*, *Geophys. Monogr. Ser.*,

vol. 29, edited by J. E. Hansen and T. Takahashi, pp. 130–163, AGU, Washington, D. C.

Hansen, J., G. Russell, A. Lacis, I. Fung, D. Rind, and P. Stone (1985), Climate response times: Dependence on climate sensitivity and ocean mixing, *Science*, *229*, 857–859.

Knutson, T. R., T. L. Delworth, I. M. Held, R. J. Stouffer, K. W. Dixon, D. Schwarzkopf, G. Stenchikov, and V. Ramaswamy (2006), Assessment of twentieth-century regional surface temperature trends using the GFDL CM2 coupled models, *J. Clim.*, *19*, 1624–1651.

Manabe, S., R. J. Stouffer, M. J. Spelman, and K. Bryan (1991), Transient responses of a coupled ocean-atmosphere model to gradual changes of atmospheric CO_2: part 1: Annual mean response, *J. Clim.*, *4*, 785–818.

Meehl, G. A., W. M. Washington, W. D. Collins, J. M. Arblaster, A. Hu, L. E. Buja, W. G. Strand, and H. Teng (2005), How much more global warming and sea level rise?, *Science*, *307*, 1769–1772.

Nakicenovic, N., and R. Swart (Eds.) (2000), *Special Report of the Intergovernmental Panel on Climate Change*, pp. 570, Cambridge Univ. Press, New York.

Raper, S. C. B., J. M. Gregory, and R. J. Stouffer (2002), The role of climate sensitivity and ocean heat uptake on AOGCM transient temperature response, *J. Clim.*, *15*, 124–130.

Russell, J. L., R. J. Stouffer, and K. W. Dixon (2006a), Intercomparison of the southern ocean circulations in IPCC coupled model control simulations, *J. Clim.*, in press.

Russell, J. L., K. W. Dixon, A. Gnanadesikan, R. J. Stouffer, and J. R. Toggweiler (2006b), The Southern Hemisphere westerlies in a warming world: Propping open the door to the deep ocean, *J. Clim.*, in press.

Sarmiento, J. L., T. M. C. Hughes, R. J. Stouffer, and S. Manabe (1998), Simulated response of the ocean carbon cycle to anthropogenic climate warming, *Nature*, *393*, 245–249.

Stouffer, R. J. (2004), Time scales of climate response, *J. Clim.*, *17*, 209–217.

Stouffer, R. J., et al. (2006), GFDL's CM2 global coupled climate models: part IV: Idealized climate response, *J. Clim.*, *19*, 723–740.

Vecchi, G. A., B. J. Soden, A. T. Wittenberg, I. M. Held, A. Leetmaa, and M. J. Harrison (2006), Weakening of tropical Pacific atmospheric circulation due to anthropogenic forcing, *Nature*, *441*, 73–76.

Winton, M. (2000), A reformulated three-layer sea ice model, *J. Atmos. Oceanic Technol.*, *17*, 525–531.

J. Russell, Biogeochemical Dynamics Laboratory, Department of Geosciences, University of Arizona, 1040 E. 4th St., Gould-Simpson Building, Rm. 317, Tucson, AZ 85721, USA.

M. J. Spelman and R. J. Stouffer, Geophysical Fluid Dynamics Laboratory, Princeton University, Forrestal Campus, 201 Forrestal Road, Princeton, NJ 08540–6649, USA. (ronald.stouffer@noaa.gov)